Multiple Controllers for Trajectory Tracking of a Nonlinear SISO System

TargetDeLab Technical Paper 04

TargetDeLab Group

2026

Abstract

Trajectory tracking of the nonlinear system $\dot{x} = x^2 + u$ is studied using seven control structures: a two-level switching PID, bang-bang control, feedforward/PID, static PID, PI2D2, variable-gain PID, and the compensator K(s+z)/[s(s+p)]. The common-plant comparison is deliberately broad: all seven controllers are exercised on the same nonlinear plant so that differences in accuracy, control effort, noise sensitivity, saturation behavior, and implementation complexity arise from controller structure rather than from a changing benchmark. $J_u = \int_0^T u^{\mathsf{T}}(t)u(t)\,dt$ is used as a quadratic control-effort measure rather than as physical energy without an additional actuator model; $u_{\text{ff}} = \dot{r} - r^2$ is the exact feedforward input for perfect tracking and not a universal energy lower bound; The simulations were repeated with dt=10 microseconds, x(0)=0.1, and deterministic 40 dB noise. The results confirm that direct differentiation of a noisy reference drives control effort dramatically upward, whereas filtering reduces it by roughly three orders of magnitude. Bang-bang control exhibits low quadratic effort but much worse accuracy and therefore cannot be called “optimal” without explicit weighting of the accuracy-effort trade-off.

1 Introduction and Literature Context

Compensation of a known nonlinearity by state feedback/feedforward is directly connected to input-output feedback linearization. For systems with actuator limits, saturation materially changes the closed-loop dynamics and requires dedicated anti-windup treatment. The literature has demonstrated both the usefulness of feedback linearization for SISO tracking and the need to handle input constraints explicitly. This chapter does not claim a new general stability theorem; it presents a controlled numerical comparison of specific controller structures.

1.1 Controller Comparison as a Multi-Objective Problem

Comparing controllers is meaningful only after the performance objectives and admissible constraints are stated. In tracking problems, small error, low control effort, limited peak actuation, robustness to uncertainty, noise sensitivity, and implementation complexity can conflict. A controller that minimizes one metric can perform poorly on another. The appropriate interpretation is therefore multi-objective: the set of non-dominated designs forms a Pareto frontier, and selecting a controller requires an application-dependent weighting or constraint specification rather than a universal ranking [7-9].

The quadratic quantity $J_u = \int_0^T u^{\mathsf{T}}(t)u(t)\,dt$ is widely used as a mathematical measure of control activity. It becomes physical energy only when the actuator model makes uTu proportional to power. In electrical, hydraulic, thermal, and mechanical actuators the physical energy may depend on additional states, efficiencies, voltages, currents, flows, forces, velocities, or losses. This chapter therefore retains J_u as a reproducible control-effort metric and avoids assigning it an unsupported physical interpretation.

1.2 Feedforward, Feedback, and Two-Degree-of-Freedom Structure

Feedforward and feedback solve complementary problems. If the plant model and desired trajectory are known, feedforward can supply the nominal input required to produce that trajectory. Feedback then corrects initial-condition errors, disturbances, and model mismatch. A two-degree-of-freedom architecture separates these roles and can improve tracking without forcing the feedback loop to generate the entire reference-dependent control action [7,10].

For the exactly known plant $\dot{x} = f(x) + u$, the feedforward term $\dot{r}$-f(r) reproduces the reference trajectory when x=r. It is a trajectory-specific inverse input, not an optimal-control solution unless a separate optimization problem is posed and solved. The distinction matters because different admissible trajectories, tracking tolerances, and actuator constraints define different optimization problems.

1.3 Sensitivity, Robustness, and the Meaning of Fair Comparison

In classical feedback theory, the sensitivity function is S(s)=1/(1+L(s)) for loop transfer L(s), and the complementary sensitivity is T(s)=L(s)/(1+L(s)). These functions quantify disturbance rejection, robustness, and measurement-noise transmission for an LTI loop. In a nonlinear closed loop, analogous robustness questions must be formulated through local linearization, induced gains, incremental stability, simulation ensembles, or other explicitly defined nonlinear measures [7-8].

Fair controller comparison also requires identical initial conditions, reference signals, integration tolerances, actuator limits, noise realizations, and metric definitions. Where a method internally differentiates a noisy signal, the numerical differentiator or filter is part of the controller implementation and must be included in the comparison. The methodology in this chapter follows this reproducibility principle.

1.4 Saturation and Constraint-Aware Nonlinear Control

Input constraints can invalidate the nominal cancellation on which feedback-linearizing controllers rely. Once the actuator saturates, the commanded virtual input can no longer be realized and the linearized error dynamics cease to describe the actual plant. Anti-windup, reference governors, and constraint-aware predictive controllers are established strategies for managing this mismatch [2-3,11]. In the present comparison, saturation is retained as an explicit scenario so that controller ranking is not based only on unconstrained nominal behavior.

2 Model and Theoretical Formulation

Common controller-comparison topology. Every candidate C0-C6 receives the same reference and operates on the same nonlinear plant. Scenario-dependent noise, filtering, actuator saturation, and switching constraints are applied at the indicated conditioning points so that comparisons use identical external conditions.

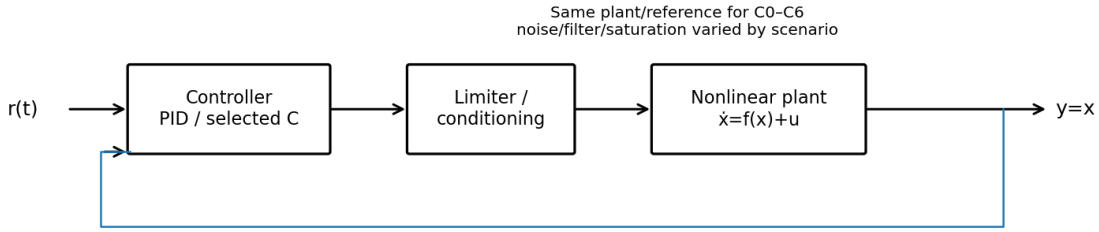


Figure 27. Control topology used in Chapter 4.

The plant is

$\dot{x}(t)$ = f(x(t)) + u(t), f(x)=x^2, y(t)=x(t).

With e(t)=r(t)-x(t), the structure is chosen as

u(t) = -f(x(t)) + $\dot{r}(t)$ + v(t).

Then $\dot{x}$=$\dot{r}$+v and therefore $\dot{e}$=-v. Thus the known nonlinearity is cancelled exactly only in the unsaturated, exactly modelled system. For v=0 and x(0)=r(0), the exact feedforward input is $u_{\text{ff}} = \dot{r} - r^2$. The quantity $J_{\text{ff}} = \int_0^T u_{\text{ff}}^2(t)\,dt$ is the effort associated with this particular perfect trajectory; it is not a universal minimum-energy lower bound for arbitrary controllers or for tracking with nonzero error.

For a fair optimization, either the constrained formulation min $J_u = \int_0^T u^2(t)\,dt$ subject to RMSE $\leq \varepsilon_R$, $|e(T)| \leq \varepsilon_T$, and $|u| \leq u_{\max}$, or the composite criterion J=ISE+λ_u J_u is used. Minimizing J_u without a tracking constraint is methodologically inadequate because it favors weak or zero control action.

3 Controllers

Table 16. Controllers evaluated in Section 4.3.

ID	Structure	Description
C0	Two-level switching PID	Switches between high and reduced PID gains according to the tracking condition, combining aggressive recovery with milder action near the desired trajectory.
C1	Bang–bang	Applies $u = +A_{BB}$ when $x < r$ and $u = -A_{BB}$ when $x > r$; A_{BB} is the controller switching amplitude and is distinct from the separate actuator ceiling used in S4–S5.
C2	Feedforward + switching PID	u=$\dot{r}$-r^2+v_{PID}.
C3	Static PID	u=-x^2+$\dot{r}$+Kp e+Kd $\dot{e}$+Ki$\int$e.
C4	PI2D2	Generalized PID-type law augmented with a second integral and a second derivative term, providing additional low-frequency accumulation and high-frequency shaping degrees of freedom.
C5	Variable-gain PID	Error-dependent PID gains, here increased with $\lvert e \rvert$ and bounded above, so the controller acts more aggressively for large deviations and softens as the trajectory approaches the reference.
C6	Compensator/integrator	C(s)=K(s+z)/[s(s+p)].

The seven structures span deliberately different control philosophies. C0 changes PID authority by switching between two gain levels; C1 uses only the sign of the tracking error and therefore trades precision for bounded, simple action; C2 combines model-based trajectory feedforward with feedback correction; C3 is the fixed-gain nonlinear-cancellation PID baseline; C4 extends that baseline with second-order integral/derivative action; C5 adapts the effective PID gains as the error magnitude changes; and C6 represents a dynamic compensator with an integrator and a pole-zero shaping pair. Evaluating all seven on the same plant and reference exposes these structural trade-offs under identical numerical conditions.

4 Simulation Scenarios

Simulation time is 0-1 s, dt=10^{-5} s, x(0)=0.1. The reference is r=2.5 sin(2 pi 5t) for t<0.5 s and then holds its final value. Noise is 40 dB AWGN with a fixed seed for reproducibility. The filter reproduces the repeated two-point smoothing used by the code. In S4-S5, $|u| \leq 150$ is imposed. In S5, 10 ms dwell/hysteresis is imposed on the dynamic switching controllers.

Table 17. Results and parameters.

Scenario	Noise	Filter	|u| limit	Hysteresis
S1	No	No	No	No
S2	40 dB	No	No	No
S3	40 dB	Yes	No	No
S4	40 dB	Yes	150	No
S5	40 dB	Yes	150	10 ms

5 Numerical Results

5.1 Scenario 1

Scenario definition. Clean reference tracking: no added noise, no filter, no actuator limit, and no hysteresis/dwell constraint. All controllers C0-C6 use T=1 s, Δt=10^{-5} s, x(0)=0.1, and r(t)=2.5 sin(2 pi 5t) for t<0.5 s, after which the reference is held at its final value.

Table 18. Scenario 1 results.

C	IAE	ISE	RMSE	J_u	Peak |u|	Sat. %
0	0.0006349	1.909e-05	0.004375	1535	78.54	0.00
1	0.3078	0.2915	0.54	2114	46.55	0.00
2	0.0006062	1.874e-05	0.004335	1535	78.54	0.00
3	0.001304	3.573e-05	0.005982	1535	78.54	0.00
4	0.001254	3.148e-05	0.005615	1535	78.54	0.00
5	0.001161	3.298e-05	0.005747	1535	78.54	0.00
6	0.04436	0.002859	0.05347	1550	78.79	0.00

Minimum RMSE: C2 = 0.004335. Minimum J_u: C4 = 1535. The two rankings do not necessarily coincide, confirming that accuracy and control effort must be evaluated simultaneously.

Scenario 1 establishes the unconstrained accuracy-effort baseline. C2 gives the smallest tracking error, whereas C4 gives the smallest quadratic control effort, so the controller selected as “best” changes with the objective. This is the central comparison principle used in the remaining scenarios: RMSE measures trajectory fidelity, while J_u measures actuator demand, and neither metric alone captures the complete design trade-off.

For visual legibility, Figures 30–34 plot only the representative subset C0, C1, C3, and C5. C0 represents switched PID behavior, C1 the discontinuous bang–bang extreme, C3 the fixed-gain PID baseline, and C5 the variable-gain PID family. C2 and C4 track very closely to the high-accuracy PID-family curves at the scale of these plots, while C6 is numerically summarized in the tables; plotting all seven simultaneously would obscure rather than clarify the trajectory differences. All seven controllers remain included in every quantitative table and ranking.

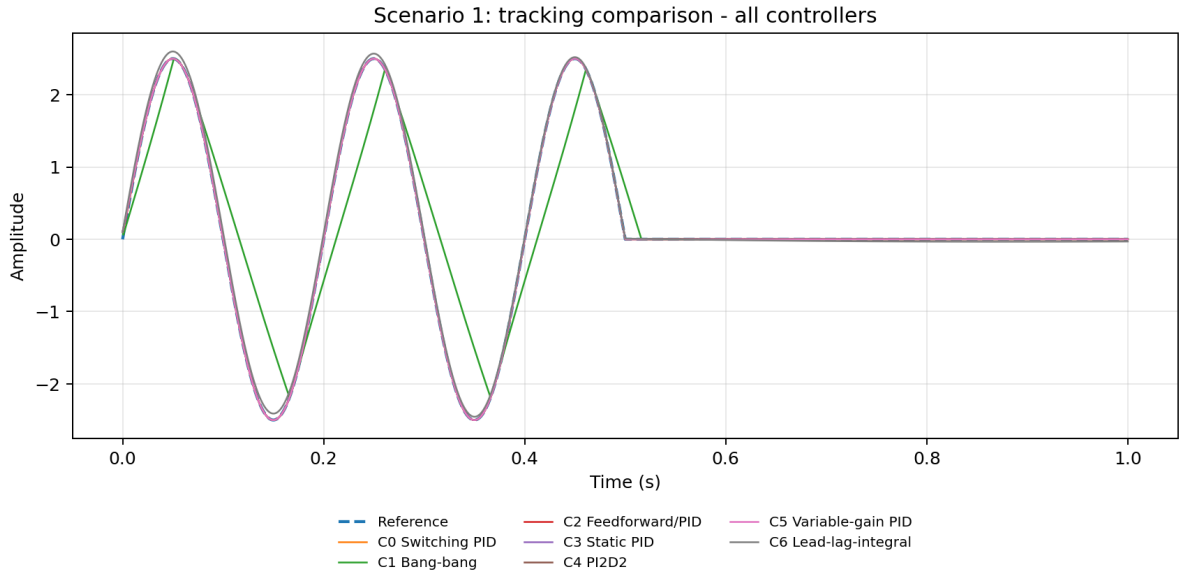


Figure 30. Tracking comparison for Scenario 1; all controllers C0–C6 are shown.

5.2 Scenario 2

Scenario definition. Scenario 1 is repeated with 40 dB AWGN and no filtering. This deliberately exposes the sensitivity of controller structures that numerically differentiate the noisy reference/measurement signals.

Table 19. Scenario 2 results.

C	IAE	ISE	RMSE	J_u	Peak |u|	Sat. %
0	0.0009142	2.338e-05	0.004839	3.134e+06	8723	0.00
1	0.3254	0.3086	0.5555	2114	46.55	0.00
2	0.0008878	2.323e-05	0.004823	3.134e+06	8723	0.00
3	0.001093	2.51e-05	0.005014	3.133e+06	8723	0.00
4	0.001051	2.211e-05	0.004706	3.133e+06	8723	0.00
5	0.0009868	2.36e-05	0.004862	3.133e+06	8723	0.00
6	0.03718	0.002009	0.04482	3.133e+06	8722	0.00

Minimum RMSE: C4 = 0.004706. Minimum J_u: C1 = 2114. The two rankings do not necessarily coincide, confirming that accuracy and control effort must be evaluated simultaneously.

With unfiltered measurement/reference noise, the ranking changes and the control-effort penalty becomes a dominant issue for structures containing numerical differentiation. The result shows that nominal clean-signal performance is not sufficient for controller selection. A controller that is accurate in Scenario 1 can become impractical when high-frequency noise is differentiated, even if the state trajectory itself still appears acceptable.

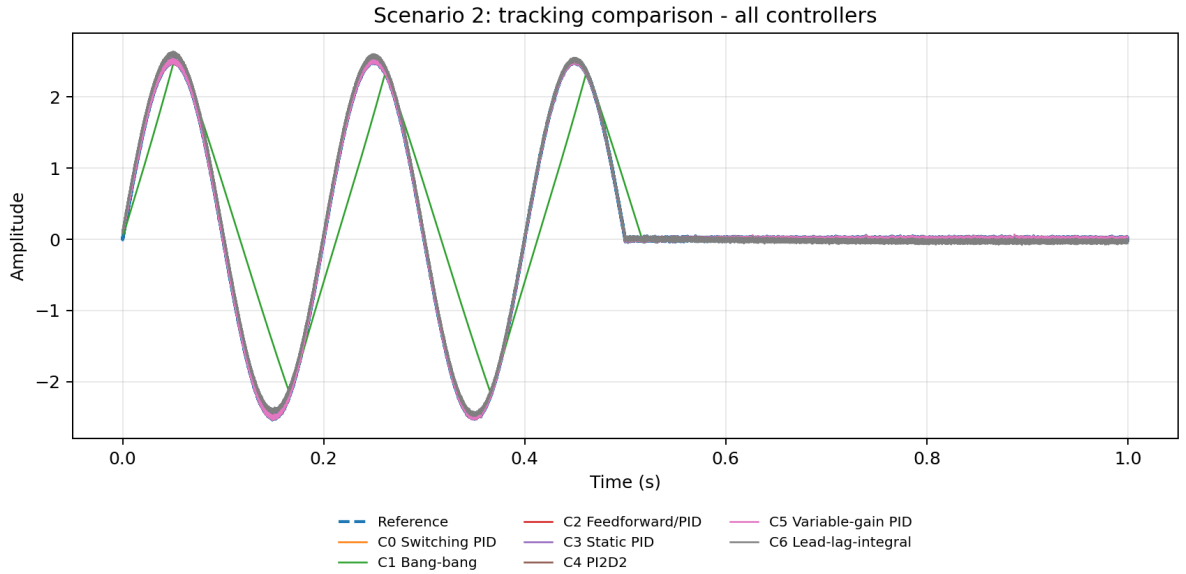


Figure 31. Tracking comparison for Scenario 2; all controllers C0–C6 are shown.

5.3 Scenario 3

Scenario definition. The 40 dB AWGN of Scenario 2 is retained, and the repeated two-point smoothing implemented is enabled. No actuator saturation is imposed. The comparison therefore isolates the effect of filtering under the same noisy excitation.

Table 20. Scenario 3 results.

C	IAE	ISE	RMSE	J_u	Peak |u|	Sat. %
0	0.0007161	2.201e-05	0.004697	6171	325	0.00
1	0.3124	0.2967	0.5447	2114	46.55	0.00
2	0.0006863	2.165e-05	0.004659	6171	325	0.00
3	0.001302	3.56e-05	0.00597	6174	324.5	0.00
4	0.001252	3.136e-05	0.005604	6174	324.6	0.00
5	0.001159	3.286e-05	0.005737	6174	324.5	0.00
6	0.04427	0.002848	0.05337	6188	324.6	0.00

Minimum RMSE: C2 = 0.004659. Minimum J_u: C1 = 2114. The two rankings do not necessarily coincide, confirming that accuracy and control effort must be evaluated simultaneously.

Filtering restores much of the useful tracking behavior without reproducing the extreme control effort of the unfiltered noisy case. The comparison between Scenarios 2 and 3 therefore isolates the value of preprocessing: it does not change the plant, but it changes what reaches the derivative-sensitive controller terms. The result supports treating filtering as part of the implemented control architecture rather than as a cosmetic post-processing step.

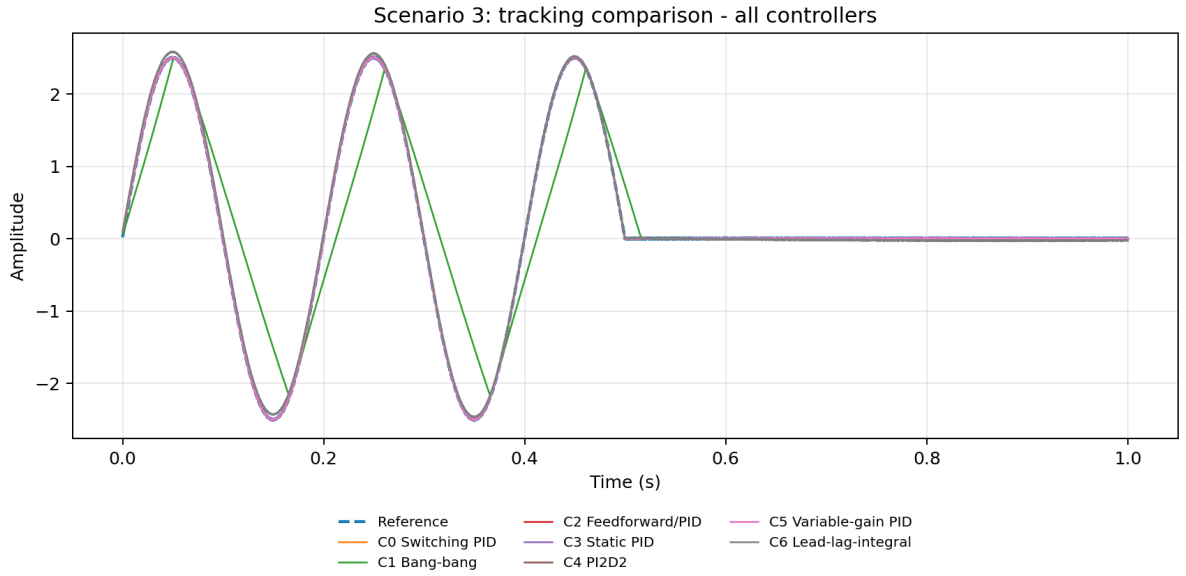


Figure 32. Tracking comparison for Scenario 3; all controllers C0–C6 are shown.

5.4 Scenario 4

Scenario definition. The filtered 40 dB noisy case is retained and the actuator command is limited to $|u| \leq 150$. No additional dwell/hysteresis constraint is imposed. Saturation percentage is reported together with tracking and control-effort metrics.

Table 21. Scenario 4 results.

C	IAE	ISE	RMSE	J_u	Peak |u|	Sat. %
0	0.02079	0.001252	0.03538	5531	150	5.85
1	0.3124	0.2967	0.5447	2114	46.55	0.00
2	0.0206	0.001232	0.0351	5529	150	5.84
3	0.01179	0.000372	0.01929	5675	150	6.17
4	0.01098	0.0003221	0.01795	5664	150	6.12
5	0.01148	0.0003498	0.0187	5673	150	6.16
6	0.07936	0.01185	0.1089	5549	150	5.73

Minimum RMSE: C4 = 0.01795. Minimum J_u: C1 = 2114. The two rankings do not necessarily coincide, confirming that accuracy and control effort must be evaluated simultaneously.

The C1 peak value 46.55 does not contradict the ± 150 actuator limit. The ± 150 value in Scenarios 4–5 is a saturation ceiling applied to the commanded actuator signal; it is not the bang–bang switching amplitude. In the implemented C1 law the bang–bang level A_{BB} produces a peak of 46.55, which lies below the actuator ceiling. Consequently C1 has 0% saturation in Tables 21–22.

Adding dwell/hysteresis to the already constrained case primarily changes the admissible switching behavior rather than the actuator bound itself. The unchanged best RMSE in the reported data indicates that the additional switching constraint

does not materially improve the best tracking value for this test, but it makes the dynamic switching implementation better defined by preventing arbitrarily rapid mode changes. Its value should therefore be judged together with switching activity and implementation robustness, not from RMSE alone.

The increase in the minimum RMSE after imposing $|u| \leq 150$ is the expected consequence of actuator authority becoming limited. Once saturation is active, the controller cannot realize the command demanded by the nominal cancellation/tracking law, so a larger tracking error is unavoidable. Reporting saturation percentage together with RMSE and J_u is therefore essential for distinguishing a controller-tuning limitation from a hard actuator constraint.

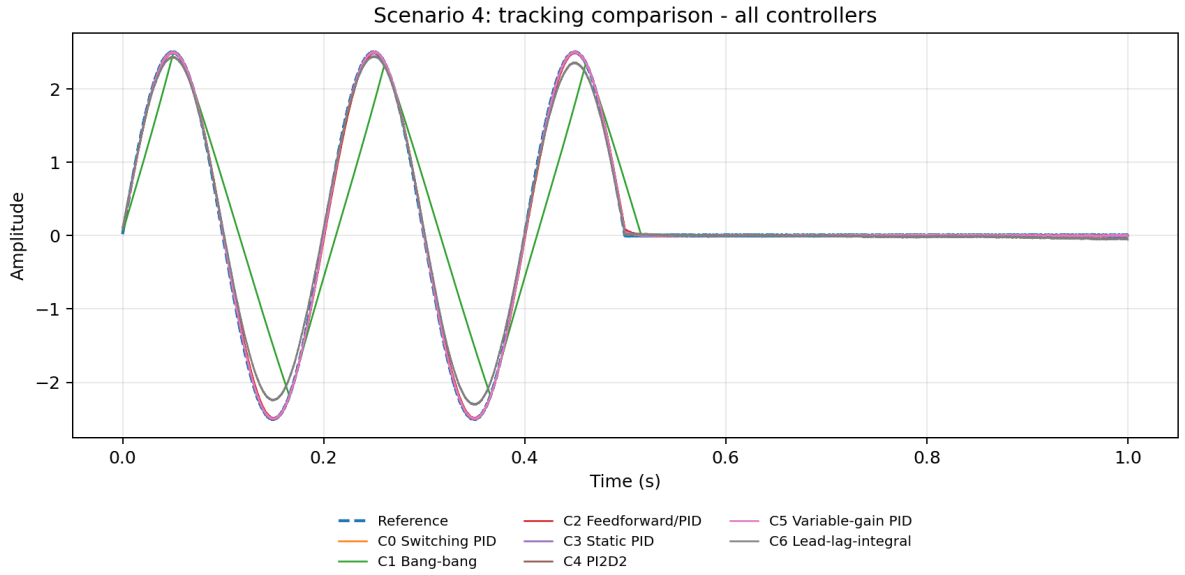


Figure 33. Tracking comparison for Scenario 4; all controllers C0–C6 are shown.

5.5 Scenario 5

Scenario definition. Scenario 4 is retained, including 40 dB noise, filtering, and $|u| \leq 150$, while a 10 ms dwell/hysteresis condition is added to the dynamic switching controllers. This scenario isolates the additional effect of constrained switching.

Table 22. Scenario 5 results.

C	IAE	ISE	RMSE	J_u	Peak |u|	Sat. %
0	0.01213	0.0004187	0.02046	5673	150	6.16
1	0.3124	0.2967	0.5447	2114	46.55	0.00
2	0.01197	0.0004094	0.02024	5673	150	6.14
3	0.01179	0.000372	0.01929	5675	150	6.17
4	0.01098	0.0003221	0.01795	5664	150	6.12
5	0.01149	0.0003524	0.01877	5673	150	6.16
6	0.07936	0.01185	0.1089	5549	150	5.73

Minimum RMSE: C4 = 0.01795. Minimum J_u: C1 = 2114. The two rankings do not

necessarily coincide, confirming that accuracy and control effort must be evaluated simultaneously.

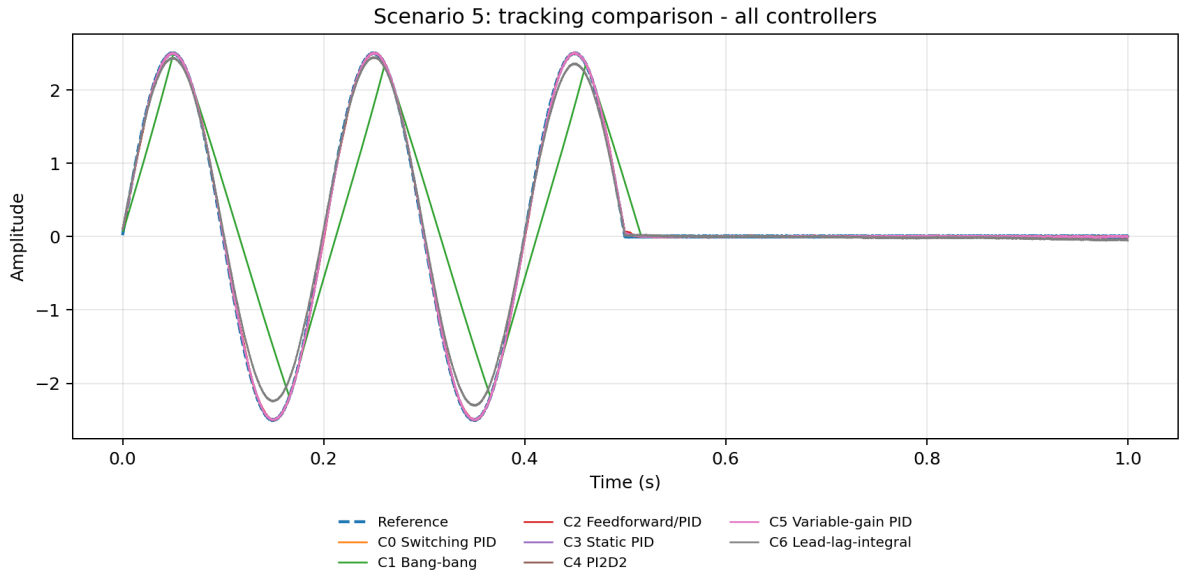


Figure 34. Tracking comparison for Scenario 5; all controllers C0–C6 are shown.

6 Principal Study Findings

For the static PID C3, unfiltered noise increases J_u from 1534.9 to 3.13e+06, approximately 2041 times. With filtering, it decreases to 6173.6, about 508 times lower than the unfiltered noisy case. The cause is direct numerical differentiation of the reference, which amplifies high-frequency content.

The C1 bang-bang controller has low J_u because its amplitude is limited, but RMSE remains approximately 0.54-0.56 in the unsaturated scenarios, two orders of magnitude worse than the PID-based controllers. A ranking based on weighted indices therefore does not justify a claim of an overall better controller.

In the constrained scenarios S4-S5, the PID-based controllers reach |u|=150 for approximately 6% of the time. No dedicated anti-windup protection is implemented in the Chapter 4 simulations. Because the integral states continue integrating during saturation, S4–S5 are baseline saturation cases rather than anti-windup designs. This is an explicit limitation of the study and should be considered when interpreting the constrained-scenario rankings.

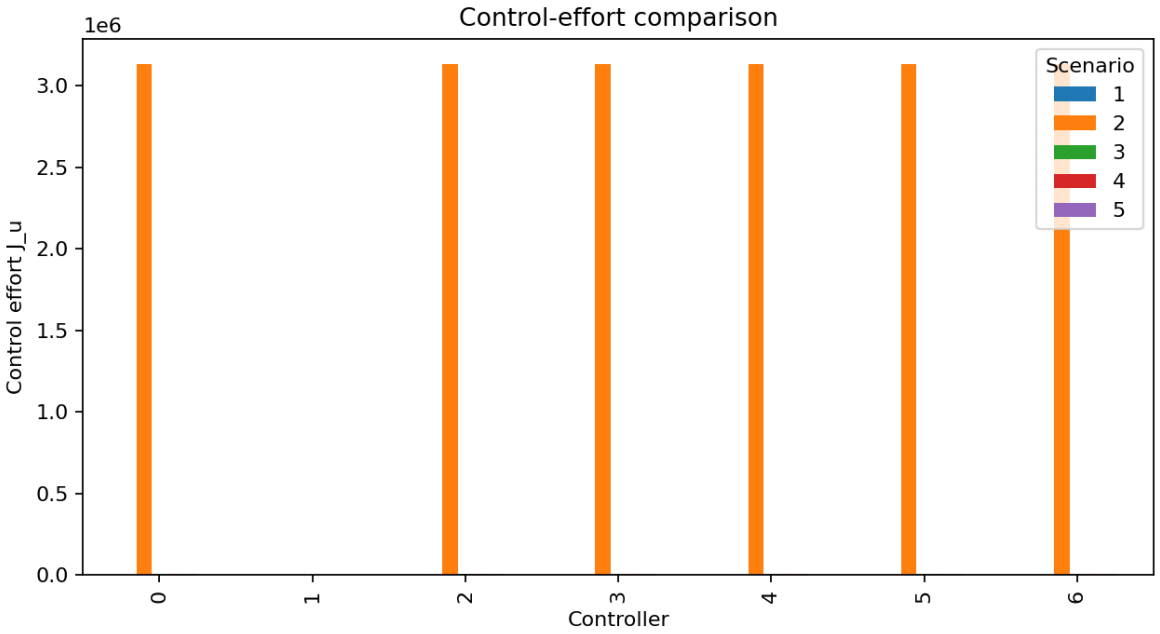


Figure 36. Quadratic control effort by controller and scenario. Each controller is compared across the five operating conditions using the same J_u definition; the figure highlights the dramatic effort increase caused by unfiltered noise in derivative-sensitive controllers, the recovery obtained by filtering, and the much lower but less accurate bang–bang effort level.

7 Conclusions

The comparative study is scientifically useful after the above corrections. The nonlinear cancellation u=-x^2+$\dot{r}$+v transforms the nominal tracking-error dynamics into $\dot{e}$=-v and explains the very high accuracy of the PID-based controllers. The principal practical drawback is dependence on $\dot{r}$: noise on the reference produces very large control effort when differentiated directly. Filtering largely restores performance. No dedicated anti-windup protection is applied in the reported saturation scenarios; a complete practical implementation should add and separately validate an anti-windup mechanism. There is no unique “best” controller without a defined multi-objective criterion. For high-accuracy applications, C3-C5 are the strongest baseline choices in the present data; where control action must be strictly limited, C1 reduces effort at the cost of a substantial loss of tracking accuracy.

The five scenarios collectively show why controller comparison must be performed under progressively realistic conditions. Clean tracking identifies nominal capability; noise exposes derivative sensitivity; filtering tests a practical mitigation; saturation introduces a hard physical constraint; and dwell/hysteresis restricts switching behavior. The rankings change across these conditions, so the chapter does not support a universal winner. Instead, it provides a structured basis for selecting a controller according to the required balance among tracking accuracy, control effort, noise sensitivity, actuator limits, and switching complexity.

Table 23. Controller-selection overview from the simulated scenarios.

Controller	Best observed role	Scenario evidence	Selection guidance
C0	High-accuracy switched PID baseline	S1–S3; constrained in S4–S5	Choose when switched gain authority is acceptable and high tracking accuracy is required.
C1	Lowest bounded control activity, simplest switching	S2–S5 minimum J_u; peak $\|u\| = 46.55$	Choose when actuation magnitude/effort dominates and substantially poorer tracking can be tolerated.
C2	Best nominal/filtered tracking in reported unconstrained cases	S1 and S3 minimum RMSE	Choose when model-based feedforward is available and trajectory accuracy is the primary objective.
C3	Robust fixed-gain reference baseline	Competitive in all scenarios	Choose for implementation simplicity and predictable PID behavior without gain scheduling.
C4	Best constrained tracking in reported data	S2, S4 and S5 minimum RMSE; S1 minimum J_u within high-accuracy family	Choose when the additional PI2D2 shaping terms are implementable and constrained accuracy is emphasized.
C5	Variable-gain compromise	Competitive S1–S5	Choose when stronger correction for large errors and softer gains near the reference are desirable.
C6	Dynamic compensator alternative	Quantified in all tables; higher RMSE than PID family	Choose primarily when the pole-zero/integrator structure matches implementation or design constraints.

This table is a decision aid for the specific simulated plant and scenarios, not a universal controller ranking. The preferred controller changes with the metric and operating constraint.

Relationship to the Complete Book

This paper is a self-contained study extracted and reformatted from the corresponding research chapter of *Nonlinear Control: From Model to Evidence*. The complete book provides the unified progression across all seven studies, cross-study synthesis, extended methodological context, and the MATLAB/Octave and Python software-companion architecture used for replication and further experimentation.

7.1 References

[1] Kravaris, C., Chung, C.-B., “Nonlinear state feedback synthesis by global input/output linearization,” AIChE Journal, 33(4), 592–603, 1987. DOI: 10.1002/aic.690330408.

[2] Kothare, M.V., Campo, P.J., Morari, M., Nett, C.N., “A unified framework for the study of anti-windup designs,” Automatica, 30(12), 1869–1883, 1994. DOI: 10.1016/0005-1098(94)90048-5.

[3] Doyle, F.J., “An anti-windup input–output linearization scheme for SISO systems,” Journal of Process Control, 9(3), 213–220, 1999. DOI: 10.1016/S0959-1524(98)00047-X.

[4] M. J. Kurtz and M. A. Henson, “Input-output linearizing control of constrained nonlinear processes,” Journal of Process Control, vol. 7, no. 1, pp. 3-17, 1997. DOI: 10.1016/S0959-1524(96)00006-6.

[5] Caparroz, M., Soltesz, K., Hägglund, T., Guzmán, J.L., “Anti-Windup in PID Control: Review, Analysis, and New Tuning Directions,” 2026.

[6] B. D. O. Anderson and J. B. Moore, Optimal Control: Linear Quadratic Methods, Prentice Hall, 1990.

[7] K. J. Astrom and R. M. Murray, Feedback Systems: An Introduction for Scientists and Engineers, Princeton University Press, 2008.

[8] S. Skogestad and I. Postlethwaite, Multivariable Feedback Control: Analysis and Design, 2nd ed., Wiley, 2005.

[9] S. Boyd and L. Vandenberghe, Convex Optimization, Cambridge University Press, 2004.

[10] J.-J. E. Slotine and W. Li, Applied Nonlinear Control, Prentice Hall, 1991.

[11] L. Zaccarian and A. R. Teel, Modern Anti-windup Synthesis: Control Augmentation for Actuator Saturation, Princeton University Press, 2011.